PTEP

Prog. Theor. Exp. Phys. **2012**, 02B009 (16 pages)
DOI: 10.1093/ptep/pts038

Secondary charged beam lines at the J-PARC hadron experimental hall

Keizo Agari[1], Shun Enomoto[2], Hiroyuki Fujioka[3], Yuya Fujiwara[4], Tadashi Hashimoto[4], Ryugo S. Hayano[4], Toshihiko Hiraiwa[3], Erina Hirose[1], Masaharu Ieiri[1], Youichi Igarashi[1], Masami Iio[1], Jun Imazato[1], Kentaro Inoue[2], Yosuke Ishiguro[3], Kenta Itahashi[5], Masahiko Iwasaki[5,6], Yohji Katoh[1], Shingo Kawasaki[2], Akio Kiyomichi[7], Hiroshi Kou[6], Michifumi Minakawa[1], Ryotaro Muto[1], Tomofumi Nagae[3], Megumi Naruki[1], Hiroyuki Noumi[8], Hiroaki Ohnishi[5], Haruhiko Outa[5], Yuta Sada[3], Fuminori Sakuma[5], Masaharu Sato[4], Yoshinori Sato[1], Shin'ya Sawada[1], Hexi Shi[4], Yoshihisa Shirakabe[1], Yoshihiro Suzuki[1], Hitoshi Takahashi[1], Toshiyuki Takahashi[1], Minoru Takasaki[1], Kazuhiro H. Tanaka[1], Makoto Tokuda[6], Akihisa Toyoda[1], Kyo Tsukada[9], Mifuyu Ukai[9], Hiroaki Watanabe[1], Takeshi O. Yamamoto[9], and Yutaka Yamanoi[1]

[1]*High Energy Accelerator Research Organization (KEK), Tsukuba, Ibaraki 305-0801, Japan*
[2]*Department of Physics, Osaka University, Toyonaka, Osaka 560-0043, Japan*
[3]*Department of Physics, Kyoto University, Kyoto 606-8502, Japan*
[4]*Department of Physics, The University of Tokyo, Bunkyo, Tokyo 113-0033, Japan*
[5]*RIKEN Nishina Center, RIKEN, Wako, Saitama 351-0198, Japan*
[6]*Department of Physics, Tokyo Institute of Technology, Meguro, Tokyo 152-8551, Japan*
[7]*Japan Synchrotron Radiation Research Institute, Sayo, Hyogo 679-5198, Japan*
[8]*Research Center for Nuclear Physics (RCNP), Osaka University, Ibaraki, Osaka 567-0047, Japan*
[9]*Department of Physics, Tohoku University, Sendai 980-8578, Japan*

Received May 31, 2012; Accepted October 2, 2012; Published November 6, 2012

Three beam lines for secondary charged particles are constructed in the hadron experimental hall of J-PARC. The K1.8 beam line, which incorporates two separators, delivers clean beams of kaons up to 2 GeV/c. The K1.8BR beam line is a branch of K1.8, for low-momentum particles up to 1.2 GeV/c. The K1.1BR beam line is a shorter line designed for low-momentum kaons. Details of these beam line designs, as well as the commissioning results, are described.

1. Introduction

In the hadron experimental hall (HD-hall) of J-PARC, two extraction lines for charged secondary particles are constructed for a single production target of the primary beam line [1].

The K1.8 beam line is designed for a spectroscopic study of Ξ hypernuclei and a systematic study of the double strangeness system via the (K^-, K^+) reaction [2,3]. Since the cross section of Ξ hyperon production in the (K^-, K^+) reaction on hydrogen is known to be maximal at 1.8 GeV/c [4], a kaon beam line with a maximum central momentum of ∼2 GeV/c is required. The K1.8BR beam line is a branch line of K1.8 to deliver kaon beams of 0.8 ∼ 1.2 GeV/c for experimental studies of Λ hypernuclei, deeply bound kaonic nuclei, and so on. The K1.1BR beam line is designed for low momentum at a 0.8 GeV/c separated kaon beam for stopped-kaon experiments.

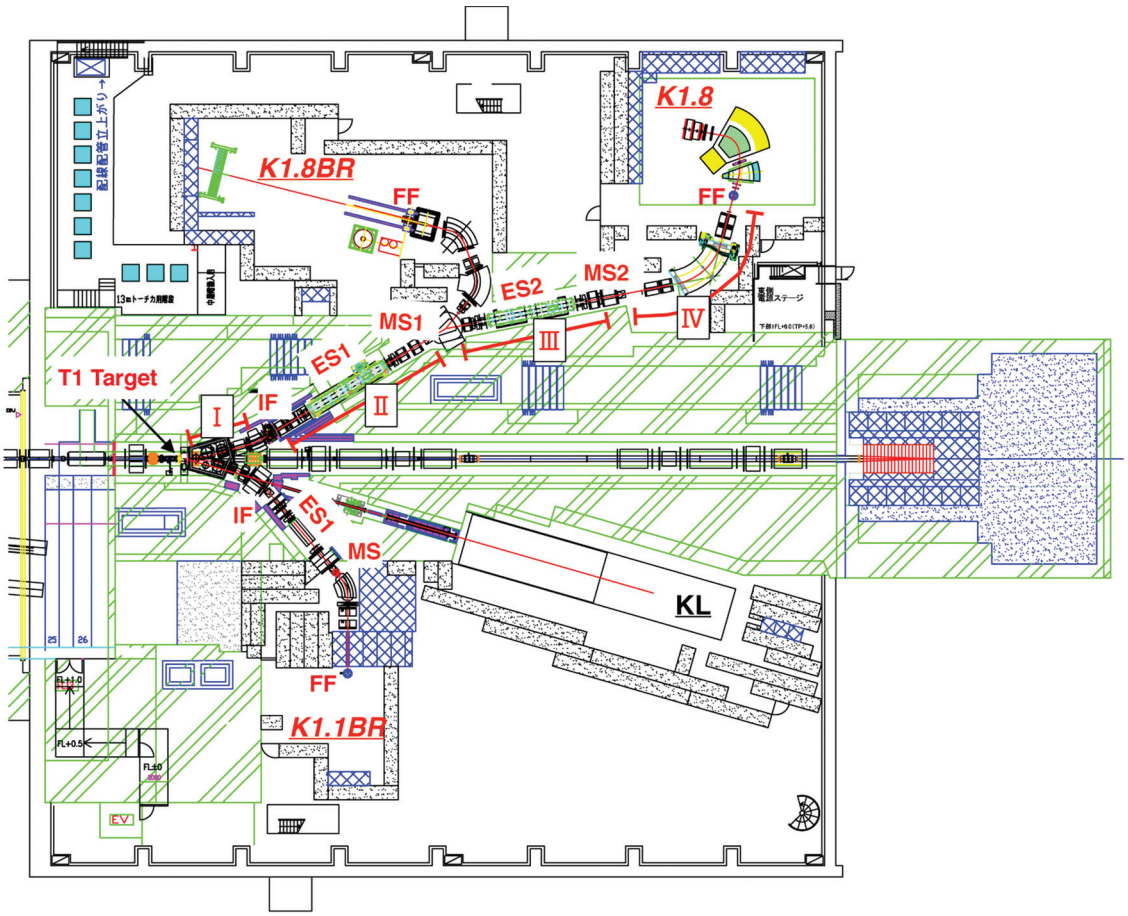

Fig. 1. Layout of the HD-hall, charged secondary beam lines (K1.8, K1.8BR, and K1.1BR), and each experimental area. I–IV along the K1.8 beam line correspond to 4 sections: the front-end section, the first mass separation section, the second mass separation section, and the beam analyzer section. 'IF', 'MS', 'ES', and 'FF' denote intermediate focus, mass slit, electrostatic separator and final focus, respectively.

These lines have been constructed for kaon beams with reduced pion contamination. The kaon beam must be purified, otherwise a few hundred times more pions are mixed in the kaon beam. With slow extracted primary protons with an expected intensity of 9 μA at 30 GeV, a K^- intensity of 10^6 per second will be delivered to the experimental area. At this expected kaon intensity, the single rate capability of tracking devices placed in the beam line is close to the limit. Since the ratio of wanted particles to unwanted particles must be better than unity, a two-stage separation is adopted for K1.8 to transport the wanted particles efficiently. This two-stage separation configuration is quite effective for purifying wanted particles; this has been demonstrated in the K4 beam line of KEK-PS [5] and the D6 beam line of BNL-AGS [6]. An intermediate focus [7] is employed for both lines to eliminate unwanted particles that come from around the production target, such as cloud pions from K^0_s decay [8].

2. K1.8 and K1.8BR beam lines

2.1. Design concept

Secondary beams produced at the T1 target are extracted from the primary beam line as shown in Fig. 1. The K1.8 beam line is composed of 4 sections (I–IV in Fig. 1): the front-end section, the

Table 1. Beam line elements of the K1.8 beam line. The element names begining 'D', 'Q', 'S', and 'O' denote dipole, quadrupole, sextupole, and octupole magnets, respectively. 'CM' is a correction magnet to compensate deflection of orbit in the electrostatic separator. The sections in the right-hand column correspond to sections I–IV in Fig. 1 (details in the text). $(y|\phi)$, $(y|y)$, $(y|\theta\phi)$, $(y|\phi\delta)$ denote beam transfer matrix elements [13,14].

Beam line element	J-PARC designation	Gap or bore/2 (cm)	Effective length (cm)	Field at pole at 1.8 GeV/c (kG)	Bend (deg)	Section
D1	5C216SMIC	8	88.46	11.846	10	
Q1	NQ312MIC	8	67.84	5.5		I
Q2	Q416MIC	10	87.04	−6.929		
D2	8D218SMIC	15	99.65	15.774	15	
IF-H	Movable horizontal slit for acceptance control					
IF-V	Movable vertical slit, $(y\|\phi) = 0$					
Q3	Q410	10	54.72	7.4		
O1	O503	12.5	15	1.		
Q4	Q410	10	54.72	−8.2		
S1	SX504	12.5	27.6	0.419		
CM1	4D604V	10	20	3.76	0.743	II
ES1	Separator	10	600	$E = -750$ kV/10 cm		
CM2	4D604V	10	20	3.76	0.743	
S2	SX504	12.5	27.6	−1.141		
Q5	NQ510	12.5	56	−7.201		
Q6	NQ610	15	57.2	8.1		
MOM	movable horizontal slit for momentum acceptance control					
MS1	movable vertical slit for K–π separation $(y\|\phi) = 0$, $(y\|y) = 0.632$, $(y\|\theta\phi) = (y\|\phi\delta) = 0$					
D3	6D330S	15	165.1	−12.696	−20	
Q7	Q408	10	47	−4.511		
O2	O503	12.5	15	0.2		
S3	SX604	15	20	−1.05		
CM3	4D604V	10	20	3.76	−0.743	III
ES2	Separator	10	600	$E = 750$ kV/10 cm		
CM4	4D604V	10	20	3.76	−0.743	
S4	SX604	15	20	0.24		
Q8	NQ512	12.5	66.8	−7.9605		
Q9	NQ518	12.5	96.2	9.8799		
MS2	movable vertical slit for K–π separation $(y\|\phi) = 0$, $(y\|y) = -0.713$, $(y\|\theta\phi) = (y\|\phi\delta) = 0$					
Q10	NQ412	10	66	9.5589		
Q11	NQ412	10	66	−7.5032		
D4	13D489	20	446.8	15.0102	64	IV
Q12	NQ412	10	66	7.6768		
Q13	NQ412	10	66	−5.2168		

first mass separation section, the second mass separation section, and the beam analyzer section. The beam line elements are listed in Table 1.

The front-end section (I) is required for extraction of secondary particles from the primary beam. The extraction angle is chosen to be 6°, where the kaon production cross section is expected to be at a maximum according to the Sanford–Wang formula [9,10]. Some of the beam line elements in the front-end section are operated in a large vacuum tank of ∼1 Pa, as described elsewhere in this volume [1]. In contrast, the first mass separation section (II) is operated in higher vacuum. A vacuum window must be placed at the end of the front-end section. The secondary beam is focused vertically at a point close to the window in order to minimize the multiple-scattering effect on the

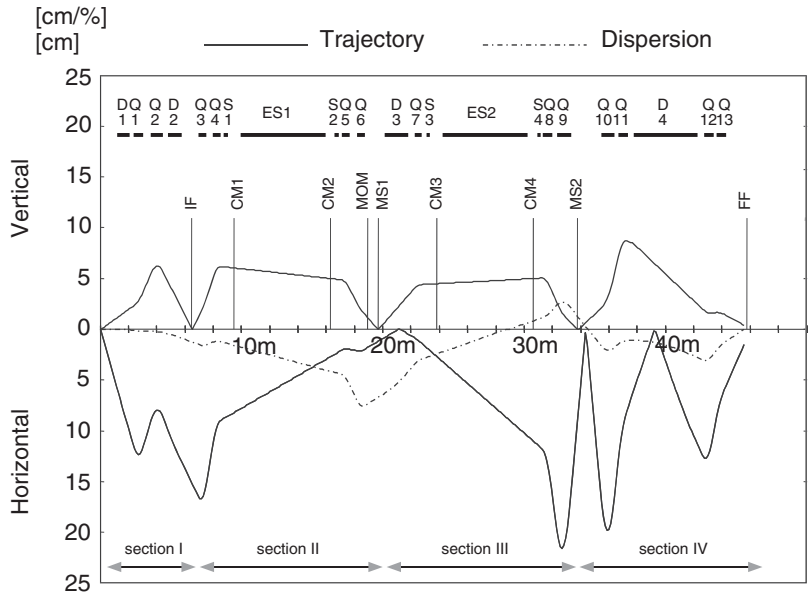

Fig. 2. The trajectories of ion optical parameters to the first order and dispersion function are shown. Four sections of the beam line are indicated.

K–π separation. A vertical slit, an IF slit, is placed at this IF plane. The K–π separation is very sensitive to the beam size at the production target. Pions from K^0_s decays and rescattered or produced at target-peripheral materials enlarge the beam size of the pion beam projected onto the production target. They are the so-called cloud pions and make the K–π separation worse [8]. The IF slit is necessary to keep the K–π separation good as it redefines the beam image at the production target.

Two electrostatic separators (ES) are employed to separate kaons from pions in the first and second mass separation sections (II and III). The details of the ES are described in Sect. 4. The beam is transported with minimum divergence in each ES, a so-called parallel beam. After ES, the beam is focused in the vertical direction at each mass slit (MS1, MS2).

A beam analyzer section (IV) with a QQDQQ magnet configuration is placed after the second mass slit, MS2. A set of tracking detectors are installed at the entrance and exit of QQDQQ in order to determine the particle trajectory and momentum. Point-to-point optics is realized between the entrance and exit of QQDQQ. The multiple scattering of a particle at the entrance and exit of QQDQQ does not affect the momentum resolution to the first-order transfer matrix. This configuration was successfully demonstrated at the K6 beam line of KEK-PS [7,11,12].

As K1.8 is too long to use a kaon beam at 1.2 GeV/c or less, K1.8BR, branching at D3 of K1.8, is designed as a shorter beam line to deliver a low-momentum separated kaon beam, as shown in Fig. 1. Although the beam time has to be shared between K1.8 and K1.8BR, preparations for experimental setups can be done independently. This is helpful for flexible and efficient coordination of experiments.

2.2. Optical calculation and expected performance of K1.8

Magnet layout and field strengths are designed using TRANSPORT [13,14]. The trajectories of first-order ion optical parameters are shown in Fig. 2. The total length of the beam line is 45.8 m. The beam is focused vertically at IF, MS1, and MS2 before the final focus point at the experimental target. A momentum slit (MOM) is placed just before MS1, where the magnitude of the dispersion

Table 2. Elements of the K1.8BR beam line (E15 option). From D1 to D3, only different values are listed, as the others are the same as those in Table 1.

Beam line element	J-PARC designation	Gap or bore/2 (cm)	Effective length (cm)	Field at pole at 1.1 GeV/c (kG)	Bend (deg)
D1			90.05	7.1115	
Q1				3.384	
Q2				−4.257	
D2				9.6396	
IF-H, IF-V	same as K1.8				
Q3				4.52	
O1				0.3	
Q4				−5.157	
S1				0.322	
CM1				2.742	0.856
ES1	same as K1.8				
CM2				2.742	0.856
S2				−1.121	
Q5				−3.862	
Q6				4.743	
MOM, MS1	same as K1.8 $(y\|\phi) = 0$, $(y\|y) = 0.844$, $(y\|\theta\phi) = (y\|\phi\delta) = 0$				
D3				7.400	20
S3	SX404	10	20	1.217	
Q7	Q306	7.5	30.34	−4.435	
D4	8D440S	20	198.9	19.3201	60
Q8	NQ410	10	46.5	−0.732	
D5	8D240S	20	195.9	17.9813	55

function is enlarged. The vertical image size at MS1 is enlarged due to higher-order aberrations. In particular, the second-order terms $(y|\theta\phi)$ and $(y|\phi\delta)$ are found to be sizable. They are eliminated by employing two sextupole magnets. In the same manner, another two sextupole magnets are employed to eliminate the second-order aberrations at MS2.

The beam after MS2 is transferred through the beam analyzer and focused onto FF. The magnet parameters and layout are tuned so as to realize point-to-point optics between the entrance and exit of the QQDQQ beam analyzer and a reasonable beam size at FF. We expect a momentum resolution of $\Delta p/p = 1.4 \times 10^{-4}$ in 1σ from the first-order transfer matrix of QQDQQ, assuming a position resolution of tracking detectors equal to 0.2 mm in 1σ. Details of the beam analyzer are described elsewhere in this volume [12].

The acceptance of the beam line is estimated to be 1.5 msr·%. Employing the Sanford–Wang formula [9,10], the intensity of negative kaons at 1.8 GeV/c is estimated to be about 7.5×10^5 particles per second, where we assume that a 54 mm thick nickel target is irradiated by a 30 GeV, 9 μA proton beam.

2.3. Optical design and expected performance of K1.8BR

The optical parameters are almost the same as those of K1.8 up to MS1. The beam line elements are listed in Table 2. The total length of the beam line is 31.3 m. A kaon beam is separated at MS1. The beam is bent to the opposite side of K1.8 at D3. After D3, the kaon beam is focused on the experimental target (FF) through a momentum analyzer. Originally, the QDQ magnet system was considered as a minimal set of the momentum analyzer up to 1.2 GeV/c, so that the beam line length can be as short as possible. A sextupole magnet (S3) is placed just before the QDQ magnets to minimize second-order aberrations in the vertical image at FF.

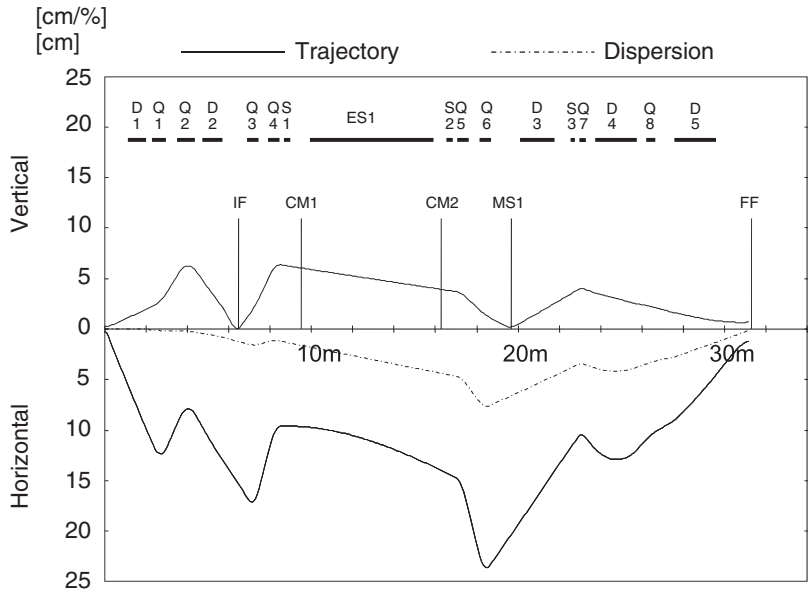

Fig. 3. First-order beam envelope of the K1.8BR for E15.

A dipole magnet D5 to change the beam direction is added after the QDQ system as required by the experimental search for a deeply bound $K^- pp$ state via the (K^-, n) reaction on ^{3}He (J-PARC E15) [15], so that an array of plastic scintillation counters can be accommodated in the experimental hall, keeping a distance of as much as 15 m from the experimental target for a precision measurement of the scattered neutron velocity. The beam envelope for this E15 option is shown in Fig. 3. The acceptance of the beam line is estimated to be 2.0 msr·%. Employing the Sanford–Wang formula [9,10] with kinematical reflection correction [16], the intensity of negative kaons at 1.1 GeV/c is estimated to be about 1.5×10^5 particles per second, where we assume that a 54 mm thick nickel target is irradiated by a 30 GeV, 9 μA proton beam.

3. K1.1BR beam line

3.1. Design concept

The K1.1BR beam line was constructed on the opposite side of the K1.8 beam line. It was originally designed by Doornbos [17] as a branch from the K1.1 beam line and shares upstream components of the beam line as K1.8BR shares components with K1.8. The current K1.1BR configuration can transport the momentum up to 1.0 GeV/c and can be used for test experiments.

3.2. Optical design and expected performance

The layout of the K1.1BR beam line is illustrated in Fig. 1, and the beam line elements are summarized in Table 3. The total length of the beam line is 21.5 m. The beam line consists of a front-end section, a mass-separation section, and a final focus section.

Secondary beams produced at the T1 target are extracted from the primary beam line with the front-end section magnets toward the opposite side of K1.8. The production angle is same as that of K1.8, and two dipole magnets D1 and D2 bend the secondary beams by 18° and 26°, respectively. As with K1.8, the IF slit is placed at the end of the front-end section, and a thin vacuum window is inserted near the slit. Scrupulous attention was paid to the design and arrangement of the front-end magnets of the beam line. The first bending magnet D1 is very close to that of the K1.8 beam line,

Table 3. List of magnets of the K1.1BR beam line. The values of the field strength are for 1.0 GeV/c settings.

Beam line element	J-PARC designation	Gap or bore/2 (cm)	Effective length (cm)	Field at pole at 1.1 GeV/c (kG)	Bend (deg)
D1	6C216SMIC	10	93	11.3	18
Q1	NQ408MIC	20	51	4.9	
Q2	NQ508MIC	25	52	−7.6	
D2	10D420MIC	20	117.2	12.9	26
IF-H	Movable horizontal slit for acceptance control				
IF-V	Movable vertical slit, $(y\|\phi) = 0$				
Q3	Q508	25	52.2	8.9	
O1	O603	30	21.8	0	
Q4	Q508	25	52.2	−8.9	
S1	SX604	30	30.4	−0.8	
ES1	Separator	10	200		
S2	SX604	30	30.4	−0.5	
Q5	NQ608	30	44.1	−10.7	
Q6	NQ608	30	44.1	11.5	
MS1	Movable vertical slit for K–π separation $(y\|\phi) = 0$, $(y\|y) = 0.389$, $(y\|\theta\phi) = (y\|\phi\delta) = 0$				
D3	8D230S	12.4	157.7	14.8	40
HFOC	Movable horizontal slit for horizontal focus at FF				
Q7	Q510	25	51.7	−9.6	
Q8	Q510	25	51.7	10.7	

and critical field interference might occur between the two C-shaped dipole magnets. By adopting a special slanting saddle coil shape, the field interference was reduced to an acceptable level (about 10% at maximum), and the charges and momenta of both beam lines can be selected with slight modification to the designed values of D1 [18]. In addition, since the K1.1BR beam line is across the KL beam line [19] as shown in Fig. 1, D1, as well as the other three magnets, Q1, Q2, and D2, were carefully designed so as not to disturb the KL beam.

In the mass-separation section, secondary beams are purified with a crossed-field-type electrostatic separator, ES1. Unwanted beams are deflected along ES1 and filtered by MS1. Two sextupole magnets are installed to eliminate second-order aberrations at MS1. In order to achieve better K–π separation, a horizontal focus slit, HFOC, is employed downstream of MS1 and a bending magnet D3.

Finally, the beams are focused on an experimental target with a doublet of quadrupole magnets. In the current configuration, the focal length of the focusing magnets is longer than that in Doornbos's design. This is due to the field limitation of the magnets in focusing 1.0 GeV/c beams, and also due to the radiation shielding of the experimental area. In paticaular, the second issue is quite important for test experiments performed at K1.1BR, because the shielding enables beam users to access their experimental devices frequently without stopping the primary beam.

Figure 4 shows the beam envelope of K1.1BR calculated with TRANSPORT [13,14]. As mentioned above, the secondary beams are focused vertically at IF and MS1 and horizontally at HFOC before the final focus point, FF. Parallel beams are made along the separator. The acceptance of the beam line is estimated to be 5.0 msr·%. Employing the Sanford–Wang formula [9,10] with kinematical reflection correction [16], the intensity of negative kaons at 0.8 GeV/c is estimated to be about 1.6×10^5 particles per second, where we assume that a 54 mm thick nickel target is irradiated by a 30 GeV, 9 μA proton beam.

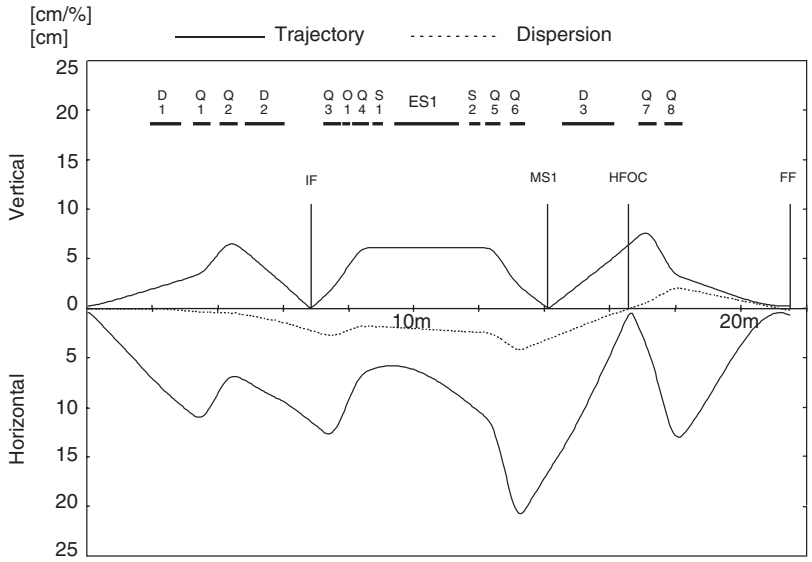

Fig. 4. First-order beam envelope of the K1.1BR beam line.

4. Electrostatic separators

An electrostatic separator (ES) is one of the key elements of a secondary beam line; it generates a transverse electric field along the beam axis to separate particles of the same momentum by their mass differences.

K1.8 is a double-stage separating beam line. Each ES of K1.8 generates an electric field in the 10 cm gap between parallel electrode plates with a size of 30 cm in width and 6 m in length. The cathode plates are made of anodized aluminum and the anodes of stainless steel. The surface flatness of the plates and the parallelism of the cathode and anode plates are within ± 0.5 mm at the maximum for a plate area of 30 cm by 6 m.

The first-stage separator (Fig. 5) in the K1.8 beam line was newly designed with several improvements in its radiation-proofing and high electric field mitigation. High-voltage power generators of Cockcroft–Walton type are mounted on the stainless steel vacuum chamber of the ES, and are directly connected to the electrodes inside the chamber. The sheath of the plug-shaped high-voltage feedthrough of the previous KEK-PS type separator was made of fiber-reinforced plastic (FRP), and was immersed in insulation-oil with a ceramic container. Since the upstream elements in the K1.8 beam line will be exposed to a high-radiation environment, we substitute ceramic for FRP in order to prolong the lifetime of the generators. An outer oil layer is no longer needed, so assembling and maintenance become much simpler.

We have avoided using organic materials. The vacuum seals are metal gaskets. Radiation-resistant turbo-molecular pumps and oil-free scroll pumps are used.

Several branch-pipes are arranged on the main vacuum chamber to mount high-voltage generators, to support electrodes and to attach vacuum ports and viewing ports. Flared openings were employed, so that outer branch-pipes are welded at the neck where it is flat and well apart from the electrodes. Electro-chemical polishing is performed at the final stage of manufacturing of the vacuum chamber after welding, to reduce unexpected discharge between the chamber and the electrodes. For the base of the generator's sheath and the corner of the electrode plates, shapes are carefully designed with finite element analysis to mitigate maximum electric field strength.

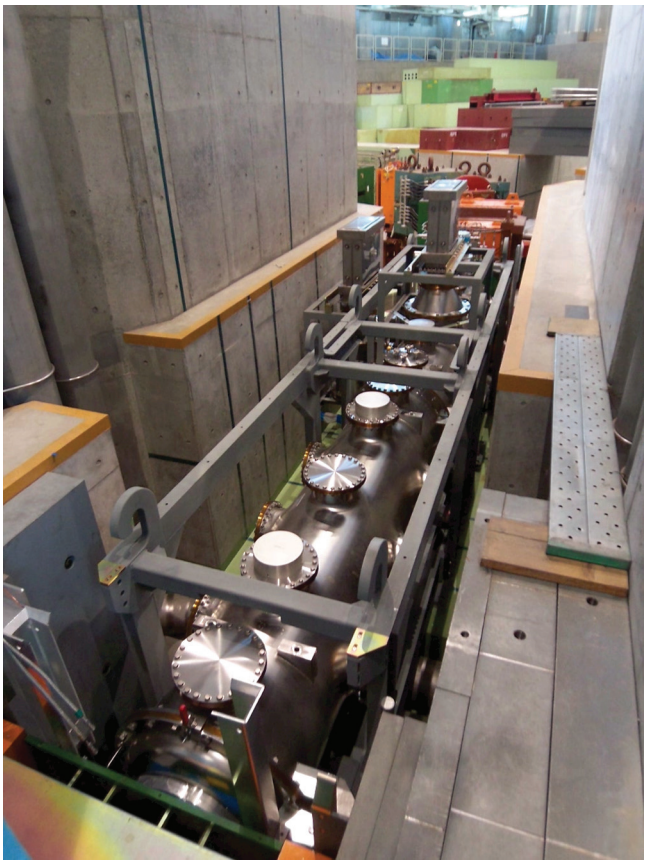

Fig. 5. The first-stage ES of the K1.8 beam line viewed from upstream.

As ES2, we reuse the existing separator, which was used for a long time at the KEK-PS K6 beam line [7], as the second stage, since the radiation level after MS1 of the K1.8 beam line is not high.

Along the K1.8 line, thin SUS foils are put downstream of the IF slit (50 μm thick) and MS1 (100 μm thick) to separate vacuum control from the low vacuum of the primary line and to realize free vacuum operation of both separators. A vacuum below 10^{-4} Pa was attained for both separators. High-voltage conditioning was performed up to about 34 kV/cm at this vacuum. Adding He(36.9%)/Ne insulating gas in the chamber up to a few times 10^{-2} Pa, the voltage was increased to a generator rating voltage of 80 kV/cm. Spark rates with leak currents beyond 10 μA were a few times per hour. We have tested the following gases: He, Ne, Ar, N_2, SF_6, and He/Ne. He/Ne gas showed a good performance as an insulating gas.

The K1.1BR has the single ES separator, which consists of 10 cm gap parallel electrodes with a size of 30 cm in width and 2 m in length. This separator is a Wien filter type with crossed magnetic field to meet the needs of the shorter beam line length for kaons at low momentum. For the K1.1 line, SUS foils of 100 μm thickness are put downstream of the IF slit and MS1 to separate vacuum control from the low vacuum of the primary line and to realize free vacuum operation from the downstream part. In Fig. 6, the orange unit on top is the high-voltage generator of the upside electrode. Cables connected from downstream are feeders for the magnet. The black pipes on the top feed cooling water for the magnetic coils. The existing separator, which has been used at the KEK-PS K5 beam line [7], is being reused after an overhaul. This separator will be replaced with a radiation-proof one.

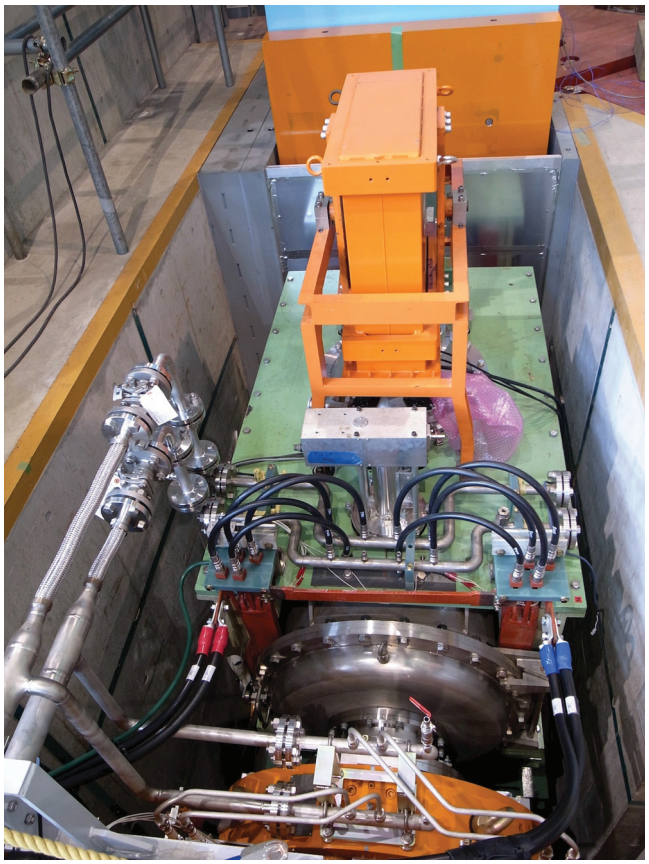

Fig. 6. The K1.1BR ES viewed from downstream.

5. Slits

5.1. Vertical slits and K/π ratio of K1.8

The shapes of three vertical slits, IF, MS1, and MS2, of the K1.8 beam line are optimized to give a better K/π ratio, not only at FF but also at MS2. A computer code, Decay TURTLE [20,21], is used to estimate the kaon yield and K/π ratio. In the estimates, the effects of multiple scattering, nuclear elastic scattering, and nuclear absorption in the slit material with a given thickness were taken into account. Multiple scattering effects at a 2.5 mm thick beryllium window placed just after the T1 target and a 50 μm thick SUS window at IF are taken into account. Third-order transfer matrix effects such as octupole magnets and fringing fields of quadrupole magnets are also taken into consideration. We assume an electric field of 75 kV/cm for each ES.

We consider a tapered jaw followed by a flat jaw, as shown in Fig. 7 (left). Gap (A) and thickness (B) of the flat jaws, the beam waist position (C), and gap (D) and thickness (E) of the tapered jaws are optimized for 1.8 GeV/c kaons. Edge scattering of unwanted particles is reduced by introducing a flat part. We confirmed the optimized shape with updated optical parameters [22]. The shape parameters for IF, MS1, and MS2 are listed in Table 4. Figure 7 (right) shows the K intensities and K/π ratios at MS2 and FF with different materials for vertical slits. Here, we assume that the pion production cross section is 30 times greater than the kaon one at 1.8 GeV/c. It is demonstrated that the WWW case (using tungsten alloy (W) for all the vertical slits) shows the best performance. In the BWW case (using brass for IF and tungsten alloy for MS1 and MS2), the expected K intensity and K/π ratio just after MS2 do not change very much.

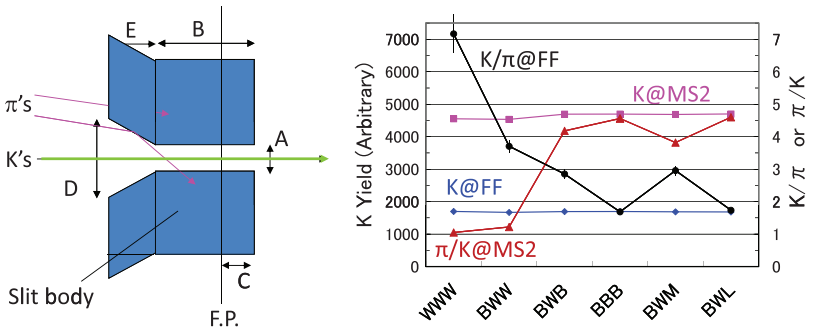

Fig. 7. Left: Cross-sectional view of a vertical slit. Parameters A to E are optimized for each vertical slit. Right: Comparison of slit performance with different materials. The alphabetic symbols on the horizontal axis represent materials used for the vertical slits, where B, L, M, and W stand for brass, lead, molybdenum, and tungsten alloy. For example, BWM means that brass, tungsten alloy, and molybdenum are used for IF, MS1, and MS2, respectively.

Table 4. Shape parameters determined for vertical slits. See Fig. 7 (left) for definitions of A to E.

	A	B	C	D	E	(mm)
IF	4	300	100	–	–	
MS1	4.7	300	100	11.1	200	
MS2	5.0	400	100	9.5	100	

5.2. Blocks used in K1.8 and K1.1 slits

The pieces of slit equipment are beam collimators or absorbers made by two or four movable heavy metal blocks. In the K1.1 and K1.8 beam lines, several types of slits have been installed. The block sizes, positions, and movable ranges of the slits are summarized in Table 5. The blocks in IF are made of brass, which is composed of 70% copper and 30% zinc, with a density of 8.5 g/cm^3 as shown in Fig. 8. The blocks of all the other slits are made of tungsten alloy, which is typically composed of 95% tungsten and few % of copper, nickel and so on, with a density of 18 g/cm^3. The tungsten alloy is non-magnetized type because the blocks are used near the magnet or between coils of the magnet. In all the slits, the blocks are driven by electric motors, and the positions of the blocks can be controlled with an accuracy of ± 0.2 mm for K1.8MOM, and ± 0.1 mm for all the other slits.

The IF slit is the most upstream slit at the first optical node point of the secondary beam. The vacuum section is also separated at this node point between the low and high vacuum sections. For the vacuum separation, a vacuum window made of stainless steel has been attached at the downstream-side flange of the IF slit. On the other hand, this window is a source of multiple scatterings of secondary particles, which may cause worse K–π separation due to possible defocusing of the beam at the mass slit. Such an effect can be minimized by focusing the beam at the vacuum window. Therefore, it is essential to locate the vacuum window close to the IF slit, where the beam is focused vertically. The horizontal IF slit is not only used as the beam collimator but is also used as a beam shutter for the personal protection system.

MS is located at the downstream end of the mass separation section and is used for particle selection. MS is a vertical-type slit to absorb unwanted secondary particles, which are spatially separated in the vertical direction by ES from wanted particles, as described in Sect. 2.1.

In addition, there are two types of horizontal slits; MOM in K1.8 is used for momentum selection of the secondary beam and is thus located at a large momentum-dispersion point. HFOC in K1.1BR is used to control beam size at the final-focus point and to suppress beam background.

Table 5. Parameters of blocks used in the slits. The 'position' column shows the approximate distance from the production target, T1, to the center of the block. Some of them are not simple rectangular-parallelepiped shapes. *The K1.1IF-V and K1.1HFOC blocks are taper-shaped on both upstream and downstream sides, the others are taper-shaped on the upstream side. In the 'movable range' column, 0 means beam axis and minus means overrun.

Name	Position from T1 (cm)	Length ×width ×height (cm^3)	Taper length (cm)	Taper angle (mrad)	Movable range of each block (cm)
K1.8IF-H	623	$20 \times 15 \times 40$	–	–	−2 to 13
K1.8IF-V	646	$30 \times 30 \times 10$	–	–	−2 to 3
K1.8MOM	1895	$10 \times 36 \times 8$	–	–	−36 to 36
K1.8MS1	1956	$50 \times 36 \times 3$	20	16	−1 to 1
K1.8MS2	3386	$50 \times 32 \times 4$	10	22	−1 to 1
K1.1IF-H	664	$20 \times 15 \times 40$	–	–	−2 to 12
K1.1IF-V	688	$30 \times 30 \times 10$	$10 + 10^*$	25	−2 to 2
K1.1MS1	1413	$40 \times 260 \times 40$	15	25	−1 to 1
K1.1HFOC	1665	$24.5 \times 50 \times 15$	$8 + 8^*$	60	−2 to 2

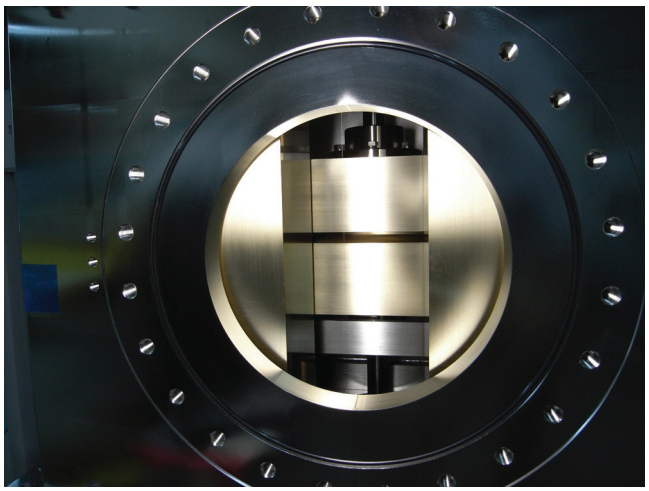

Fig. 8. Photograph of the intermediate focus slit.

6. Beam line performance

6.1. K1.8

The recent tuning and measurements of the K^- yield at the K1.8 beam line are described here. The tuning of the beam line and yield measurement were carried out for K^- in February 2012, at 1.8 GeV/c using a 3.3 kW main-ring beam (4.08×10^{12} protons/spill) and a platinum production target (50% loss target, 60 mm in length). The separator operation voltages were 50 and 40 kV/cm for ES1 and ES2, respectively, which are neither the designed nor the full operation voltages. The horizontal slits were fully opened (±130 mm for IF-H and ±180 mm for MOM) and the vertical ones were set to $-1.0/+3.0$ mm[1], ±1.17 mm, and ±1.25 mm for IF-V, MS1, and MS2, respectively.

The off-center effect from the misalignment of the slits was adjusted by offsetting the CM currents to maximize the anti-proton yield for ES1 and ES2. The best CM currents with offset for each particle

[1] This is the narrowest slit opening, since the up and down blocks of IF-V move in non-parallel alignment due to the Great East Japan Disaster. The IF-V will be replaced by a new one in the summer of 2012.

Table 6. Measured kaon yields and purity at various mass slit openings. The expected values from the decay–TURTLE simulation using the Sanford–Wang formula with kinematic reflection are also listed. 'ALL*' in the 'simulation' column indicates values for which the contribution of cloud pions from K_s^0 and muon decays is taken into account.

Slit condition		Measured		Simulation	
MS1 (mm)	MS2 (mm)	K^-(/spill)	K^-/ALL	K^-(/spill)	K^-/ALL*
±1.17	±1.25	48.1k	15.0%	44.2k	57.3%
±1.75	±1.25	51.5k	15.2%	47.7k	50.7%
±0.58	±1.25	24.4k	10.9%	16.3k	89.9%
±1.17	±1.88	57.5k	5.1%	59.3k	11.5%
±1.17	±0.63	24.4k	37.7%	13.9k	88.0%

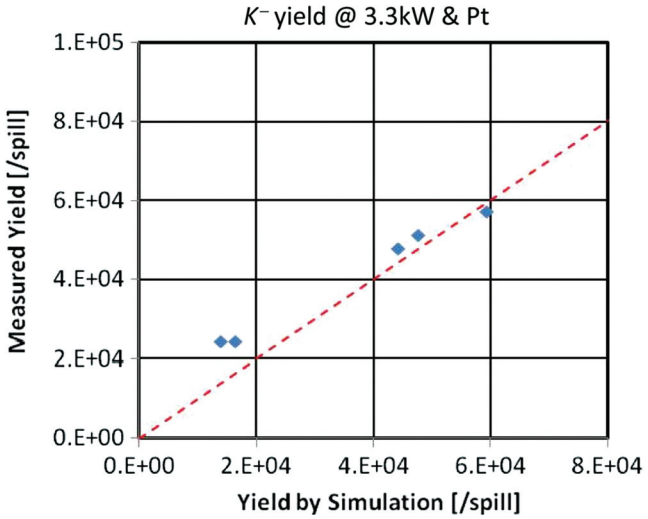

Fig. 9. The measured (vertical) and expected (horizontal) negative kaon yields for various slit conditions at a 3.3 kW main-ring beam with a platinum production target.

were also determined by scanning the CM1–4 currents. Kaon yields were evaluated by correcting the scaler counts by offline analysis. The measured yields and purity are listed in Table 6 together with the expected value from the decay-TURTLE [20,21] simulation and the cross section from the Sanford–Wang formula [9,10] with kinematical reflection. [16] In the simulation, the contribution of so-called cloud pions from K_s^0 and muon decays is taken into account, but the contribution of electrons is not. Kaon yields are well reproduced by the simulation as shown in Fig. 9. However, the kaon purity in Table 6 shows a discrepancy between the measured values and simulated ones. Further tuning of the beam optics should be performed.

6.2. K1.8BR

The K1.8BR beam line was designed to obtain a high-intensity kaon beam up to 1.2 GeV/c. Commissioning for the K1.8BR beam line has been performed since January 2009, when the first beam was delivered to the HD-hall. During the beam time in February 2012, the first trial to transport a 1.0 GeV/c beam to the final focus point was performed under the same main-ring conditions as in the previous subsection. The commissioning for 1.0 GeV/c was successfully accomplished, and optimized parameters for the spectrometer were obtained, i.e., settings for the spectrometer magnets.

Separation of particle species in secondary particles is obtained by ES1 and two correction magnets (CM1, CM2). Particle identification was performed by using two trigger counters and three

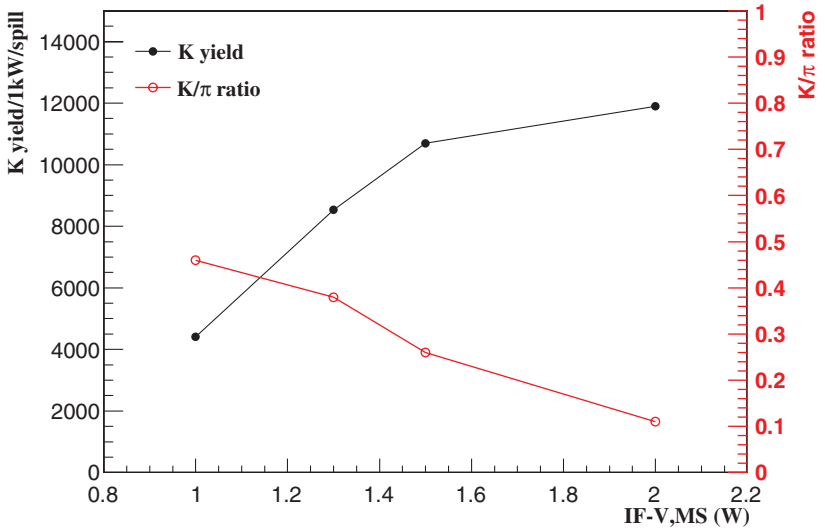

Fig. 10. The obtained 1.0 GeV/c K^- yield and K/π ratio as a function of gap distance between the IF and the MS with an ES1 field of 50 kV/cm, where the distance between the IF and the MS was adjusted with the same ratio. The width 1W is defined to be 4.0 mm vertically for the IF, and 4.7 mm for the MS. The K^- yield is normalized by a power of 1.0 kW in the main ring.

types of Cherenkov counters. Two trigger counters are installed downstream of the K1.8D3 and the K1.8BRD5 magnets, whose flight lengths are 7.7 m. Three Cherenkov counters are located downstream of the K1.8BRD5 magnet; a gas Cherenkov counter (refractive index $n = 1.002$), an aerogel Cherenkov counter ($n = 1.05$), and a water Cherenkov counter ($n = 1.33$) are used for particle identification on the trigger level. By adjusting the gap distance between IF and MS1, the kaon intensity and the K^-/π^- ratio at the final focus point of the spectrometer are successfully controlled. Typical K^- intensity and K^-/π^- ratio for the 1.0 GeV/c negative beam are achieved as 10 k/spill/kW and 0.3, respectively, as shown in Fig. 10. This K^- intensity lies between the estimations by the Sanford–Wang formula with and without kinematical correction. Further studies should be performed.

The beam profile of the kaons at the final focus point, which was reconstructed by a wire drift chamber located just before the final focus point, is shown in Fig. 11. The one standard deviation of the beam spot size at the final focus is 1.7 cm horizontally and 2.0 cm vertically. This spot size is consistent with the designed value of the beam line.

6.3. K1.1BR

The K1.1BR beam line was commissioned in October 2010, and beam tuning was performed subsequently and again in 2012 upon element realignment after the earthquake. The K^+ intensity and K^+/π^+ ratio were maximized. In order to tune the beam, several beam instruments were employed: 1) time of flight counters, 2) a Fitch-type beam Cherenkov counter to discriminate kaons and pions, 3) a beam hodoscope, 4) proportional chambers to observe the beam profile, 5) gas Cherenkov counters to trigger positrons, and 6) counters to count the beam rate. The secondary beam had 0.8 GeV/c momentum from the Pt T1 target at about 3.5 kW of slow proton beam power. ES was excited to 50 kV/cm for the beam survey and magnet setting optimization.

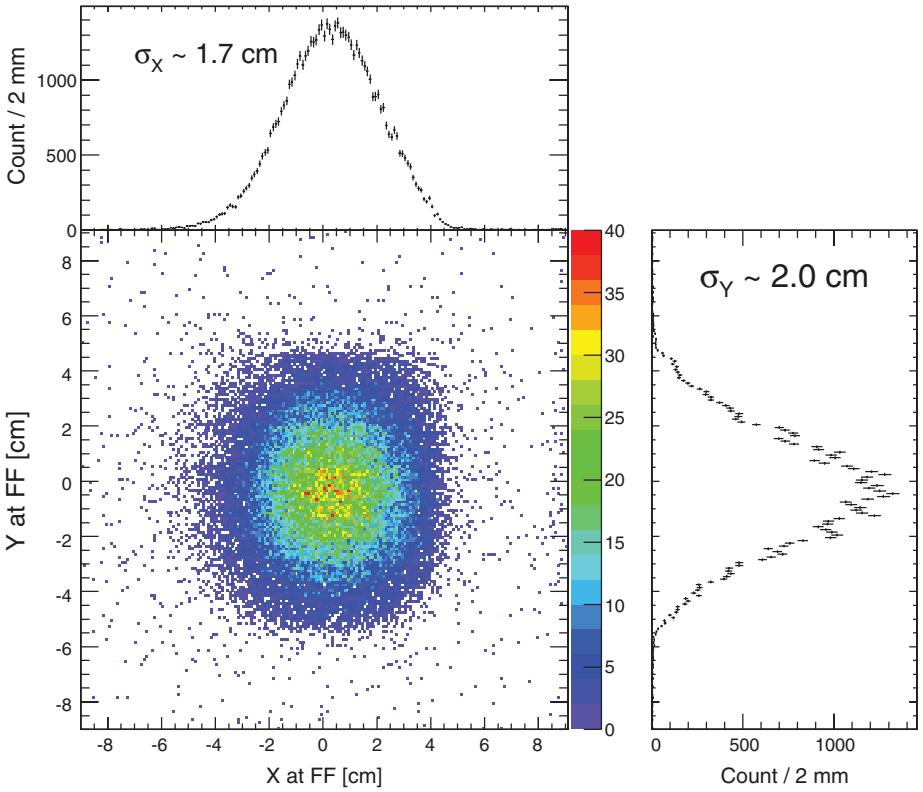

Fig. 11. Beam profile at the final focus point reconstructed by the wire drift chamber.

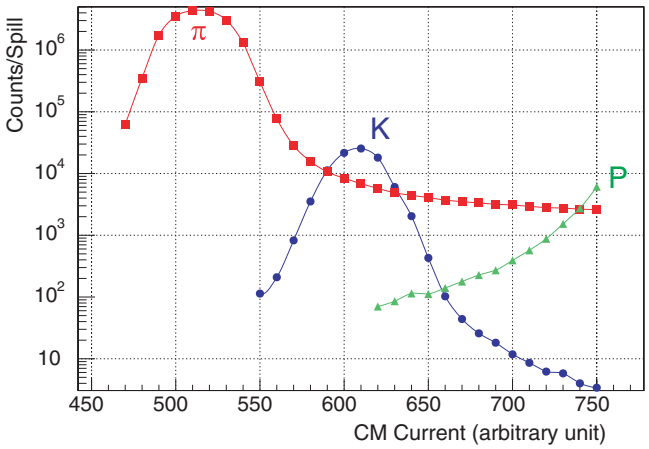

Fig. 12. K^+/π^+ separation curve of the 0.8 GeV/c beam with an ES field of 50 kV/cm.

In the kaon beam survey, the basic beam transport characteristics were confirmed in accordance with the optics design. Then, the slit openings of IF and MS were optimized by achieving the highest rate while keeping a reasonable K^+/π^+ ratio. For the so-called narrow slit settings, a kaon rate of 25 k/spill could be observed at a beam power of 3.5 kW with a good K^+/π^+ ratio of 3.7 with nearly the beam optics design values for Q3/Q4 and Q5/Q6. This K^- intensity is consistent with the Sanford–Wang formula with kinematical correction. In addition, for a wide-open slit condition, the highest kaon rate of 140 k/spill could be reached with a K^+/π^+ ratio of 0.2. Figure 12 shows the K–π separation curve at an ES field of 50 kV/cm obtained by scanning the correction

magnet (CM) current. The beam spot at the final focus was measured for the optimally tuned kaon beam at the end, and a very round profile with $\sigma_x = \sigma_y = 1.1$ cm could be observed.

7. Concluding remarks

Three beam lines, K1.8, K1.8BR, and K1.1BR, for secondary charged particles have been constructed in the J-PARC hadron experimental hall. The kaon yields and K/π ratio almost reach the expected values at each line. Since the current beam line performances were obtained under limited beam line conditions, further studies should be carried out for slit openings, finer tuning of magnets, higher separator voltages, and so forth. Several experiments [23] await an intense kaon flux with good purity under an intense primary proton beam.

Acknowledgements

We would like to express our thanks to the staff of the J-PARC accelerator, who supported our study of beam line performance. We also acknowledge several members of the experimental groups at K1.8, K.18BR, and K1.1BR, without whom our beam tuning and survey of kaons could not have been performed. We are grateful to Professor A. Yamamoto of KEK for his important advice and useful discussions for designing a new electrostatic separator. This work is partly supported by a Grant-in-Aid for Scientific Research (A) (No. 15204024) and (B) (No. 21340071).

References

[1] K. Agari et al., Prog. Theor. Exp. Phys. **2012**, 02B008 (2012).
[2] J-PARC Proposal P05, http://j-parc.jp/researcher/Hadron/en/Proposal_e.html#P05.
[3] J-PARC Proposal P07, http://j-parc.jp/researcher/Hadron/en/Proposal_e.html#P07.
[4] C. B. Dover and A. Gal, Ann. Phys. (N.Y.) **146**, 309 (1983).
[5] M. Takasaki et al., Nucl. Instrum. Methods Phys. Res., Sect. A **242**, 201 (1986).
[6] P. H. Pile et al., Nucl. Instrum. Methods Phys. Res., Sect. A **321**, 48 (1992).
[7] K. H. Tanaka et al., Nucl. Instrum. Methods Phys. Res., Sect. A **363**, 114 (1995).
[8] D. E. Lobb, Nucl. Instrum. Methods Phys. Res., Sect. A **245**, 316 (1986).
[9] J. R. Sanford and C. L. Wang, BNL-AGS internal report 11279 (1967).
[10] J. R. Sanford and C. L. Wang, BNL-AGS internal report 11479 (1967).
[11] T. Fukuda et al., Nucl. Instrum. Methods Phys. Res., Sect. A **361**, 485 (1995).
[12] T. Takahashi et al., Prog. Theor. Exp. Phys. **2012**, 02B010 (2012).
[13] K. L. Brown, F. Rothacker, D. C. Caray, and Ch. Iselin, CERN 80-04(1980).
[14] U. Rohrer, PSI Graphic Transport Framework based on a CERN-SLAC-FERMILAB version by K. L. Brown et al.
[15] J-PARC Proposal P15, http://j-parc.jp/researcher/Hadron/en/Proposal_e.html#P15.
[16] A. Yamamoto, KEK Report 81-13.
[17] J. Doornbos, Design Report (April, 2005) http://trek.kek.jp/proposal/K1.1BR.pdf, and its Addendum (May, 2007), http://trek.kek.jp/proposal/K1.1BR_add.pdf.
[18] H. Takahashi et al., to be published in IEEE Trans. Appl. Supercond.
[19] T. Yamanaka et al., '(temp) KL beam line and KOTO experiment', Prog. Theor. Exp. Phys., submitted for publication in this issue.
[20] K. L. Brown and Ch. Iselin, CERN 74-2(1974).
[21] C. Rohrer, compendium of DECAY TURTLE enhancements, PSI.
[22] Third report on technical design of the J-PARC Hadron Experimental Facility, KEK Internal report 2007-1 (in Japanese).
[23] A list of J-PARC Hadron hall experiments, http://research.kek.jp/group/nuclpart/HDeppc/Exp/.